

PPFIA1-targeting miR-181a mimic and saRNA overcome imatinib resistance in BCR-ABL1-independent chronic myeloid leukemia by suppressing leukemia stem cell regeneration

Rui Su,^{1,2,3,10} Chuting Li,^{1,2,3,10} Xiuyuan Wang,^{1,2,3,10} Zhendong Li,^{4,10} Ziqi Wen,^{1,2,3} Zhao Yin,^{1,2,3} Guiping Huang,^{1,2,3} Yanjun Liu,^{1,2,3} Juhua Yang,^{1,2,3} Haiyan Hu,^{5,6} Hong Nie,^{7,8} Keda Zhang,⁹ and Jia Fei^{1,2,3}

¹Department of Biochemistry and Molecular Biology, Medical College of Jinan University, Guangzhou 510632, China; ²Guangdong Engineering Technology Research Center of Drug Development for Small Nucleic Acids, Guangzhou 510632, China; ³Antisense Biopharmaceutical Technology Co., Ltd., Guangzhou 510632, China; ⁴Department of General Surgery, The First Affiliated Hospital of Jinan University, Guangzhou 510632, Guangdong, China; ⁵Clinical Trial Center of Shanghai Jiao Tong University Affiliated Sixth People's Hospital, Shanghai, China; ⁶Oncology Department of Shanghai Jiao Tong University Affiliated Sixth People's Hospital, Shanghai, China; ⁷International Cooperative Laboratory of Traditional Chinese Medicine Modernization and Innovative Drug Development of Chinese Ministry of Education (MOE), College of Pharmacy, Jinan University, Guangzhou 510632, China; ⁸Guangdong Province Key Laboratory of Pharmacodynamic Constituents of TCM and New Drugs Research, College of Pharmacy, Jinan University, Guangzhou 510632, China; ⁹College of Pharmacy, Shenzhen Technology University, Shenzhen 518118, China

A large proportion of patients with chronic myeloid leukemia (CML; 20%–50%) develop resistance to imatinib in a BCR-ABL1-independent manner. Therefore, new therapeutic strategies for use in this subset of imatinib-resistant CML patients are urgently needed. In this study, we used a multi-omics approach to show that PPFIA1 was targeted by miR-181a. We demonstrate that both miR-181a and PPFIA1-siRNA reduced the cell viability and proliferative capacity of CML cells *in vitro*, as well as prolonged the survival of B-NDG mice harboring human BCR-ABL1-independent imatinib-resistant CML cells. Furthermore, treatment with miR-181a mimic and PPFIA1-siRNA inhibited the self-renewal of c-kit⁺ and CD34⁺ leukemic stem cells and promoted their apoptosis. Small activating (sa)RNAs targeting the promoter of miR-181a increased the expression of endogenous primitive miR-181a (pri-miR-181a). Transfection with saRNA 1–3 inhibited the proliferation of imatinib-sensitive and -resistant CML cells. However, only saRNA-3 showed a stronger and more sustained inhibitory effect than the miR-181a mimic. Collectively, these results show that miR-181a and PPFIA1-siRNA may overcome the imatinib resistance of BCR-ABL1-independent CML, partially by inhibiting the self-renewal of leukemia stem cells and promoting their apoptosis. Moreover, exogenous saRNAs represent promising therapeutic agents in the treatment of imatinib-resistant BCR-ABL1-independent CML.

INTRODUCTION

Chronic myeloid leukemia (CML) is a cancer of the blood and bone marrow, in which BCR-ABL1 plays a central role.^{1,2} Imatinib resistance is the major incentive for developing new drugs for the treatment of CML. Furthermore, the basis for BCR-ABL-independent

drug resistance is unclear; it may be caused by (1) CML stem cells, (2) the participation of alternative survival signaling pathway, and (3) autophagy and mitochondrial metabolism. Among these, leukemic stem cells (LSCs) are the most common cause of imatinib resistance, as LSCs cannot be eradicated with imatinib.^{3,4}

MicroRNAs (miRNAs) are a class of endogenous, non-coding, single-stranded short RNAs that are involved in post-transcriptional negative regulation of genes in eukaryotes. They range in size from 19 to 24 nucleotides.⁵ They exhibit different levels of expression in various tumors and are involved in almost all aspects of tumor biology, such as proliferation, apoptosis, invasion/metastasis, and angiogenesis. Therefore, miRNAs play a prominent role in the etiology and progression of cancer.⁶ PTPRF interacting protein alpha 1 (PPFIA1), also known as liprin- α 1, belongs to the liprin family that includes liprin- α and liprin- β proteins. PPFIA1 is overexpressed in a variety of malignancies and has been

Received 20 December 2022; accepted 28 April 2023;
<https://doi.org/10.1016/j.omtn.2023.04.026>.

¹⁰These authors contributed equally

Correspondence: Haiyan Hu, Clinical trial center of Shanghai Jiao Tong University Affiliated Sixth People's Hospital, Shanghai, China.

E-mail: xuril104@163.com

Correspondence: Hong Nie, International Cooperative Laboratory of Traditional Chinese Medicine Modernization and Innovative Drug Development of Chinese Ministry of Education (MOE), College of Pharmacy, Jinan University, Guangzhou 510632, China

E-mail: hongnie1970@163.com

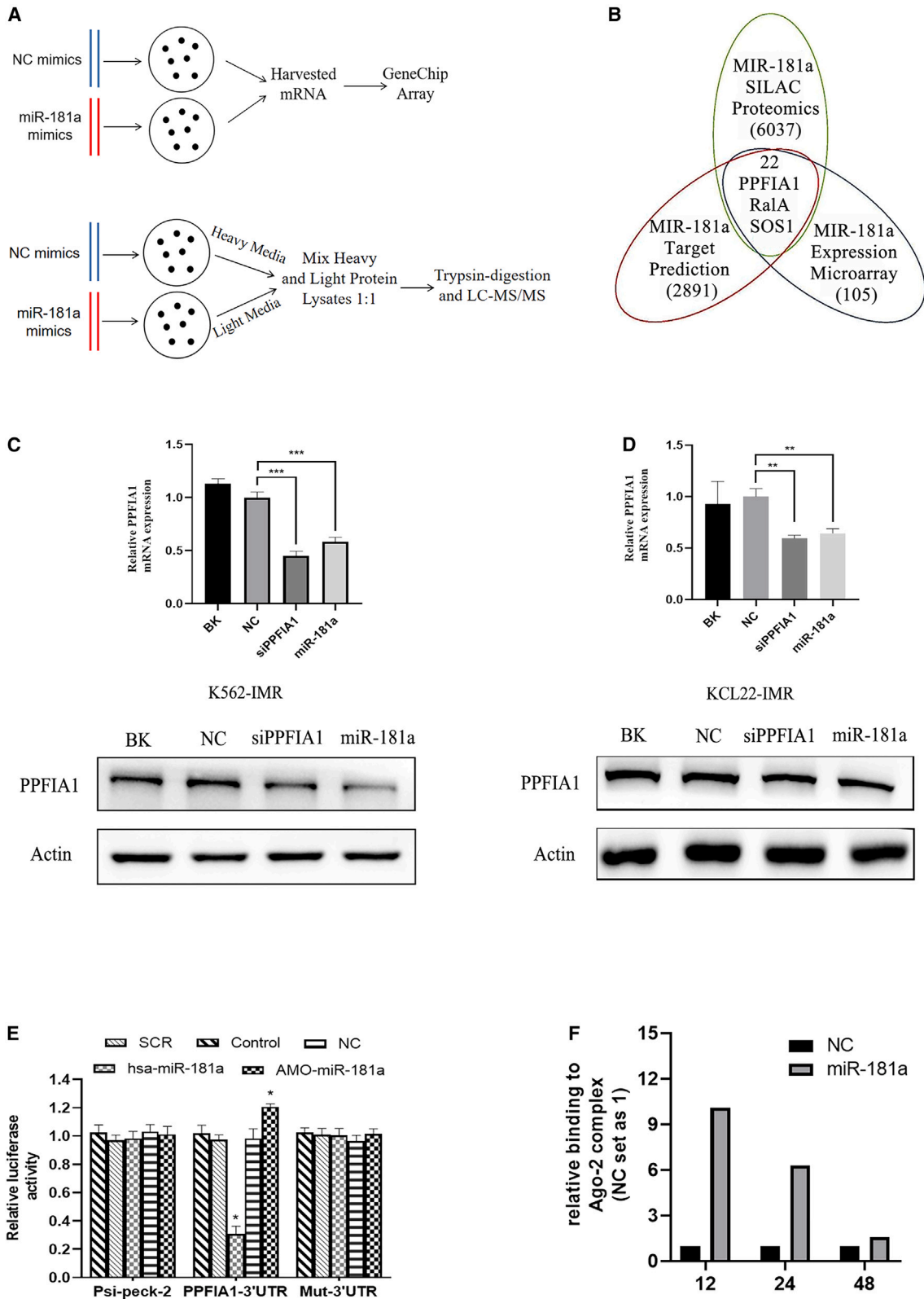
Correspondence: Keda Zhang, College of Pharmacy, Shenzhen Technology University, Shenzhen 518118, China.

E-mail: zhangkeda@sztu.edu.cn

Correspondence: Jia Fei, Department of Biochemistry and Molecular Biology, Medical College of Jinan University, Guangzhou 510632, China.

E-mail: tfiejia@jnu.edu.cn





(legend on next page)

shown to be an important promoter for tumor cells spreading in the extracellular matrix and is required for tumor cell migration and invasion, including breast cancer.⁷ We previously found by monitoring cell proliferation that miR-181a and *PPF1A1*-siRNA inhibit the development of imatinib resistance in CML. *PPF1A1* is an important gene target, and miR-181a is a promising biomarker in the prognostic prediction of hematological malignancies.^{8–11}

A considerable fraction of CML patients develop resistance to tyrosine kinase inhibitors (TKIs) because these drugs cannot kill LSCs, which leads to drug resistance and the recurrence of CML.¹² The transplantation of LSCs isolated from patients with CML into NOD-SCID mouse mice leads to leukemia development in these animals.¹³ Moreover, the biological, functional, and targeting characteristics of LSCs may be similar to those of normal hematopoietic stem cells.^{14,15} LSCs may therefore resist apoptosis and innate immune attack, while undergoing self-renewal and long-term survival.^{16,17}

Small activating RNA (saRNA), one of the dsRNAs, was initially discovered and named by Longcheng Li's team in 2006. When dsRNAs target upstream of gene promoters and control the RNA-Argonaute pathway, it is known as "RNA activation," which positively regulates the transcription of genes. It is a subsequent technology to RNAi that controls gene expression through double-stranded RNA.¹⁸ Primitive (pri)-miR-181a, induced by saRNA activation, is structurally different from the miR-181a mimic. Thus, endogenous pri-miR-181a, with a miR-181a-5p and miR-181a-3p structure, has a stronger and more durable effect on the biological functions of imatinib-resistant (IMR) CML cells than the miR-181a mimic.^{19,20}

RNA interference (RNAi) silences genes for 5 to 7 days, whereas the effects of saRNA last for up to 13 days.^{19,20} Portnoy et al. identified saRNA targets on the promoter sequence of the E-cadherin-encoding gene.²¹ Moreover, the upregulation of *DPYSL3* expression is expected to inhibit tumor metastasis and provide significant benefits for patients with locally advanced high-risk prostate cancer.^{22,23} Transfection of saRNA into hepatoma cell lines inhibits cell migration and invasion, as well as the formation of intrahepatic and distant metastasis, to prolong survival.²⁴ saRNAs upregulate cancer-related genes, regulate cell cycling and proliferation, promote cell aging and apoptosis, inhibit cancer cell invasion and migration, and reverse chemoresistance. We could harness these diverse functions of the naturally present saRNAs for use in therapeutic agents without having to synthesize potentially unsafe exogenous genetic sequences.^{25,26} Since saRNA has the same sequence form as siRNA, the delivery mode for siRNA can be applied to it. The delivery system for small nucleic acids

is now also being rapidly improved. Novel structure of ionizable lipid molecule iBL0104 enables tumor visualization therapy.²⁷ A novel ionizable lipid-assisted nucleic acid delivery system (iLAND) shows good physicochemical properties, thermal stability, and excellent siRNA transport efficiency.²⁸ Xiong et al. enhanced MAS1 expression using saRNA delivered in an amphiphilic dendrimer vector and significantly suppressed tumorigenesis and inhibited tumor progression in a variety of cancers in tumor xenograft mouse models and patient-derived tumor models.²⁹ These drug delivery systems not only solve drug issues but also significantly increase their therapeutic potential. And they allow pharmaceuticals to be given in ways that would not be conceivable otherwise.³⁰ Although, at present, the use of saRNAs in the clinic is limited, we envisage that saRNA-based therapies would benefit many patients with rare diseases.

In this study, we found that the overexpression of miR-181a mimics could overcome imatinib resistance in CML by targeting the *PPF1A1* oncogene; however, the exact mechanism was unclear. We attempted to activate endogenous pri-miR-181a expression using saRNA and compare the biological differences between CML cells with elevated pri-miR-181a or miR-181a mimic expression to explore the potential advantages of using saRNA in the treatment of IMR CML.

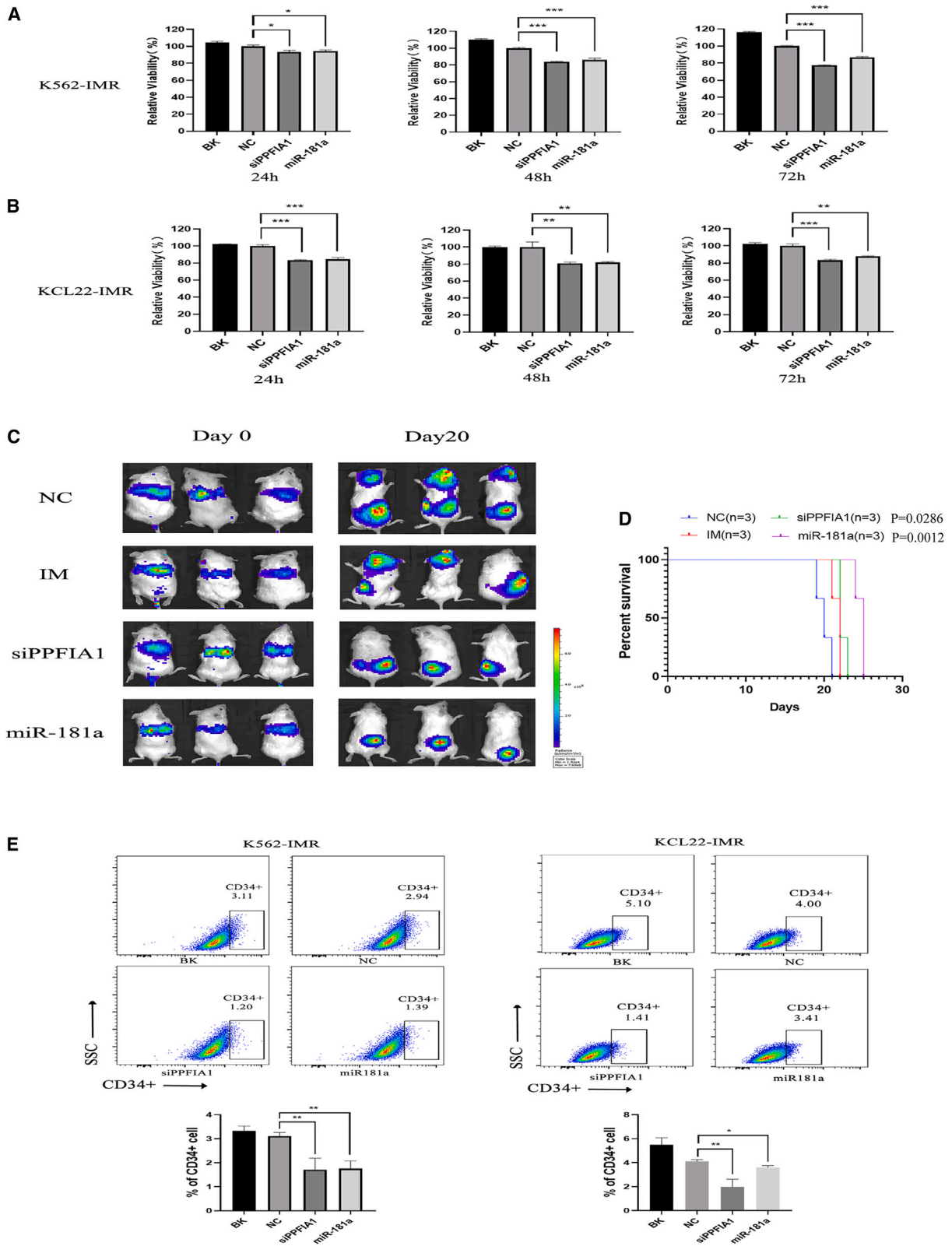
RESULTS

miR-181 targets *PPF1A1*

A schematic of microarray and SILAC quantitative proteomics workflow is shown in Figure 1A. The accuracy of target gene prediction can be greatly improved by using the combination of microarray, proteomics, and bioinformatics assays (Figure 1B). To predict the miR-181a target genes, we used the Agilent human 1A whole genome oligonucleotide chip array and measured hybridization signal intensity. We surmised that the downregulated genes could be the miR-181a target genes. We used the miRFocus software, which integrates five commonly used miRNA target gene prediction programs and analyzes the signaling pathways associated with a gene of interest. Following treatment with miR-181a mimic or the *PPF1A1*-siRNA, the expression levels of *PPF1A1* mRNA and protein were reduced in K562-IMR cells (Figure 1C) and KCL22-IMR cells (Figure 1D). *PPF1A1* 3' non-coding region (UTR) and mutants were amplified by PCR and inserted into the psiCHECK-2 vector plasmid (Promega) downstream of the fluorescein gene termination codon by double digestion (Figure 1E). miR-181a and the constructed reporter vector were co-transfected into cells using the Dual-Luciferase Reporter Assay System (E1910) (Promega). Equal amounts of the anti-Ago2 antibody were added to the miR-181a mimic and negative control (NC) groups and were used to show that Ago2 was bound to the

Figure 1. *PPF1A1* is an miR-181a target

(A) Schematic outlining the SILAC-LC-MS/MS and RIP analysis process. (B) Candidate miR-181a target genes were identified by a multi-omics approach, combining mRNA expression profiling (RIP), SILAC quantitative proteomics, and miRFocus bioinformatics prediction. (C) The expression of *PPF1A1* mRNA and protein was reduced after transfecting the miR-181a mimic and *PPF1A1*-siRNA into K562-IMR (D) or KCL22-IMR (E) cells. Luciferase reporter assay shows the interaction between miR-181a and the 3' UTR of *PPF1A1*. (F) Equal amounts of the anti-Ago2 antibody were added to the miR-181a mimic (100 nM) and NC groups (100 nM). Binding of *PPF1A1* mRNA to miR-181a was detected at 12, 24, and 48 h. The RIP assay showed that miR-181a targeted *PPF1A1* and inhibited its expression. The data are presented as the mean \pm SD, obtained from at least three independent experiments. Significance was determined by Student's t test, * $p < 0.05$, ** $p < 0.01$, versus the NC group.



(legend on next page)

miRNA. The binding between *PPFIA1* mRNA and miR-181a was detected at 12, 24, and 48 h (Figure S1). The RNA immunoprecipitation (RIP) assay showed that miR-181a targeted and inhibited *PPFIA1* expression (Figure 1F).

PPFIA1*-siRNA and miR181a inhibit the proliferation of CML cells with BCR-ABL1-independent imatinib resistance *in vitro* and *in vivo

The effects of the miR-181a mimic and the *PPFIA1*-siRNA on the viability of K562-IMR and KCL22-IMR cells were detected following transfection. K562-IMR and KCL22-IMR cells were treated with the same concentrations of the miR-181a mimic or *PPFIA1*-siRNA for 24, 48, or 72 h (Figures 2A and 2B). After culturing for a specified time, the viability of the K562-IMR and KCL22-IMR cells was measured using the CCK-8 assay. We found that the optimal duration of miR-181a mimic and *PPFIA1*-siRNA treatment was 24–96 h. The miR-181a mimic and *PPFIA1*-siRNA had strong inhibitory effects on the proliferation of K562-IMR and KCL22-IMR cells at 48 and 72 h. The K562-IMR cells were infected with a lentiviral vector containing the luciferase reporter gene, and the resulting K562-IMR/luciferase cells were cultured with puromycin (6 µg/mL) and maintained for 1 week. The K562-IMR/luciferase cells were plated into a white, opaque 96-well plate. We confirmed that the number of K562-IMR/luciferase cells was proportional to the fluorescence intensity (Figures S2A and S2B), indicating that the K562-IMR/luciferase cells could be tracked in B-NDG mice. Thus, B-NDG mice were injected with 1×10^6 K562-IMR/luciferase cells via the tail vein and imaged on day 0 mice to confirm the presence of K562-IMR/luciferase cells. The leukemic B-NDG mice were then injected with miR-181a mimic or *PPFIA1*-siRNA every other day for a total of seven times. On completion of the treatment course (day 20), we performed *in vivo* imaging of the B-NDG mice in each group to detect the proliferation of K562-IMR/luciferase cells (Figure 2C). Compared with the NC group, the fluorescence intensity (representing the severity of disease) of the B-NDG mice treated with either miR-181a mimic or *PPFIA1*-siRNA was reduced, while their survival was increased (Figure 2D). These results indicate that the miR-181a and *PPFIA1*-siRNA attenuated BCR-ABL1-independent CML resistance in B-NDG mice *in vivo*.

miR-181a mimic and *PPFIA1*-siRNA overcome BCR-ABL1-independent CML resistance by targeting c-kit⁺ CD34⁺ LSCs

The resistance of resistant CML strains to therapeutic drugs may be due to the self-renewal ability of their LSCs. Although LSCs account

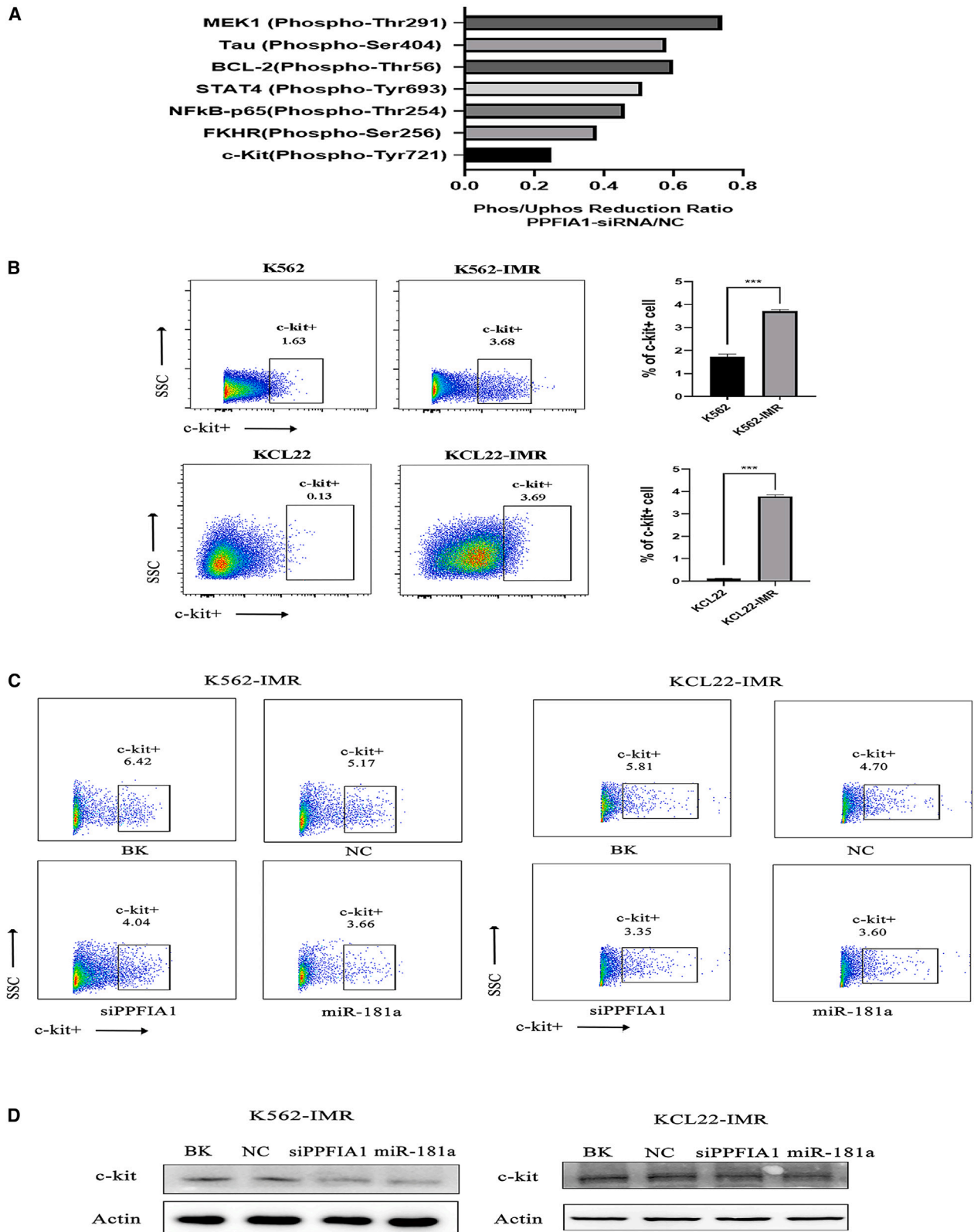
for only a small proportion of leukemia cells, their stem cell characteristics are the root of CML recurrence. The regulation of reversible protein phosphorylation plays an important role in cellular homeostasis. After transfecting *PPFIA1*-siRNA into K562 and KCL22 cells, we extracted total protein and detected by phosphorylated proteins using a phosphorylation antibody chip. We found that the phosphorylation levels of a variety of proteins were reduced following the transfection of *PPFIA1*-siRNA. Among these proteins, the levels of c-kit, a surface marker of hematopoietic cells, decreased most significantly (Figure 3A). Flow cytometry also validated that the proportion of c-kit⁺ cells in IMR populations was higher than that in the imatinib-sensitive strains of K562 and KCL22 (Figure 3B). The proportion of c-kit⁺-expressing cells was reduced after the K562-IMR and KCL22-IMR cells were treated with miR-181a mimic or *PPFIA1*-siRNA (Figure 3C). To verify whether *PPFIA1* expression had an effect on c-kit protein levels, the miR-181a mimic and *PPFIA1*-siRNA were transfected into cells, and the amount of c-kit protein was quantified by western blotting. We found that the transfection of miR-181a mimic and *PPFIA1*-siRNA reduced the expression of c-kit in cells (Figure 3D). To further study the relationship among LSCs, the miR-181a mimic, and *PPFIA1*-siRNA, we also measured CD34 expression by flow cytometry. We found that the proportion of IMR K562 and KCL22 cells expressing CD34⁺ cells was higher than that of their imatinib-sensitive equivalents (Figures S3A and S3B). However, the proportion of CD34⁺ K562-IMR and KCL22-IMR cells decreased after they were treated with miR-181a mimic and *PPFIA1*-siRNA (Figure 2E). These results suggest that the miR-181a mimic and *PPFIA1*-siRNA inhibit the proliferation of K562-IMR cells and KCL22-IMR cells by specifically targeting CD34⁺ LSCs.

saRNA-3 activates endogenous miR-181a and inhibits CML cell proliferation

We used bioinformatics to interrogate the promoter region of the miR-181a-encoding gene and designed saRNAs. Figure 4A shows the sequences of the three saRNAs (named saRNA 1–3) that we designed to target miR-181a. Compared with the BK control group, the average inhibition rates were as follows: 16.40% for the NC group, 26.56% for the miR-181a group, 25.60% for the saRNA-1 group, 25.96% for the saRNA-2 group, and 33.43% for the saRNA-3 group (Figure 4B). In K562 cells, the inhibitory effect of saRNA-3 was stronger than that of the miR-181a mimic. After transfection with saRNA1–3 for 72 h, the expression levels of endogenous miR-181a in K562 cells were detected. Out of the three saRNAs, only saRNA-3 increased the

Figure 2. The miR181a mimic and *PPFIA1*-siRNA inhibited the proliferation of chronic myeloid leukemia cells with BCR-ABL1-independent imatinib resistance *in vitro* and *in vivo*

(A) K562 and KCL22 are imatinib-sensitive cells, whereas K562-IMR and KCL22-IMR are imatinib-resistant (IMR) cells. The two IMR cell lines were cultured with increasing concentrations of imatinib, and their proliferation was measured after 48 h of imatinib treatment. (B, C) Effect of the miR-181a mimic and *PPFIA1*-siRNA (100 nM) transfection on K562-IMR and KCL22-IMR cells. Cell viability was detected using the CCK-8 assay at 24, 48, and 72 h. The miR181a mimic and *PPFIA1*-siRNA can overcome imatinib resistance in CML. (D) K562-IMR/luciferase cells were injected into the tail vein of B-NDG mice. Different groups of these B-NDG mice were then treated equal volumes of imatinib solution and 10 nmol NC, 10 nmol miR-181a mimic, or 10 nmol *PPFIA1*-siRNA every other day for 10 days. The proliferation of the K562-IMR/luciferase cells in B-NDG mice in each treatment group was then observed by *in vivo* imaging (n = 3 per group). (E) Survival analysis showed that both miR-181a and *PPFIA1*-siRNA prolonged the survival of B-NDG mice transplanted with K562-IMR/luciferase cells and treated with equal volumes of imatinib and 10 nmol NC, 10 nmol miR-181a mimic, or 10 nmol *PPFIA1*-siRNA. The data are presented as the mean ± SD, obtained from at least three independent experiments. Significance was determined by Student's t test, *p < 0.05, **p < 0.01, ***p < 0.01 versus the NC group.



(legend on next page)

expression of endogenous miR-181a (Figure 4C). We therefore next transfected cells with saRNA-3 and assessed protein expression by western blotting. In K562 cells, the PPFIA1 protein expression level was lower following miR-181a transfection, compared with the NC group (Figure 4D). We then set out to compare the effects of direct endogenous miR-181a activation or transfection with the miR-181 mimic on the proliferation of K562 cells at 72, 96, 120, and 144 h after transfection (Figure 4E). The inhibitory effect of saRNA-3 on the proliferation of K562 cells was stronger than that of the miR-181a mimic. At 120 and 144 h, the effect of the miR-181a was not statistically significantly different from that of the NC group. However, saRNA-3 had a statistically significant effect at these time points, compared with NC group. This experiment showed that saRNA-3 inhibited K562 cell proliferation for a longer time. The proliferative capacity of K562 cells was examined using the soft agar colony formation assay. After colony formation, crystal violet staining was used to identify clones, which were then counted. The K562 cells transfected with saRNA-3 formed fewer clones than the NC group (Figure 4F). These results show that saRNA-3 inhibited the proliferation of K562 cells.

saRNA-3 increases endogenous miR-181a levels to overcome the imatinib resistance of CML cells *in vitro* and *in vivo*

Regarding the inhibitory effect of saRNA-3 in IMR CML cell lines, we found that the saRNA-3 inhibited the proliferation of K562-IMR and KCL22-IMR cells more strongly than the miR-181a mimic (Figure 5A). Moreover, the expression of endogenous miR-181a was higher in the K562-IMR and KCL22-IMR cells transfected with saRNA-3 than in those transfected with the NC (Figure 5B). Western blotting indicated that saRNA-3 significantly reduced PPFIA1 protein expression in K562-IMR and KCL22-IMR cells (Figure 5C). As for the imatinib-sensitive cell lines, the proliferative ability of K562-IMR and KCL22-IMR cells was examined by soft agar colony formation assay. saRNA-3-transfected K562-IMR and KCL22-IMR cells formed fewer clonal colonies than the NC group, while there was little difference between the BK and NC groups (Figure 5D). Leukemic B-NDG mice were injected with saRNA-3 a total of seven times over the treatment period. On completion of the treatment course (day 20), *in vivo* imaging of the two groups of B-NDG mice was performed to detect the proliferation of K562-IMR/luciferase cells. Compared with the NC group, B-NDG mice injected with saRNA-3 exhibited lower fluorescence intensity, reduced disease severity (Figure 5E), and a slower rate of weight loss. Moreover, the mice in the saRNA-3 treatment group had longer survival times (Figure 5F). These results suggest that saRNA-3 inhibited the degree of

proliferation of BCR-ABL1-independent IMR CML cell lines in B-NDG mice. A summary diagram outlining the regulatory network discussed above is presented in Figure 6.

DISCUSSION

TKIs are effective drugs in the early treatment of CML. However, patients with CML can develop resistance to imatinib. To date, no effective drugs have been developed to treat the full range of IMR CML variants.³¹ Moreover, 20%–50% of CML patients develop BCR-ABL1-independent imatinib resistance, which may be caused by LSCs. Thus, it is of utmost importance to develop new drugs to treat BCR-ABL1-independent IMR CML.³²

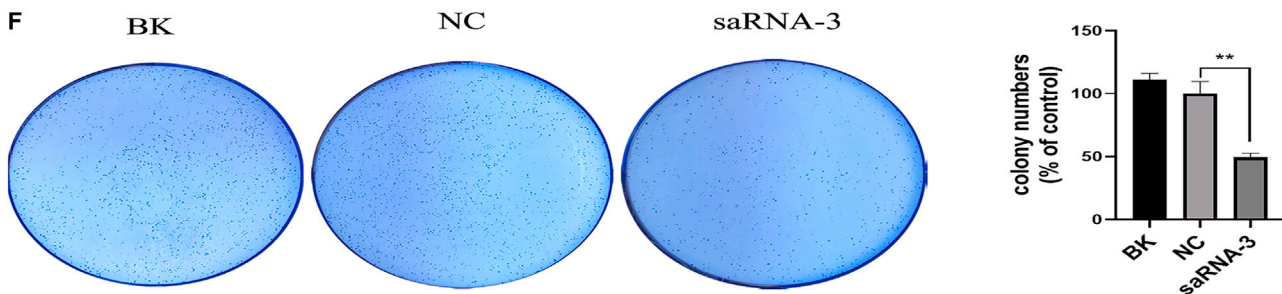
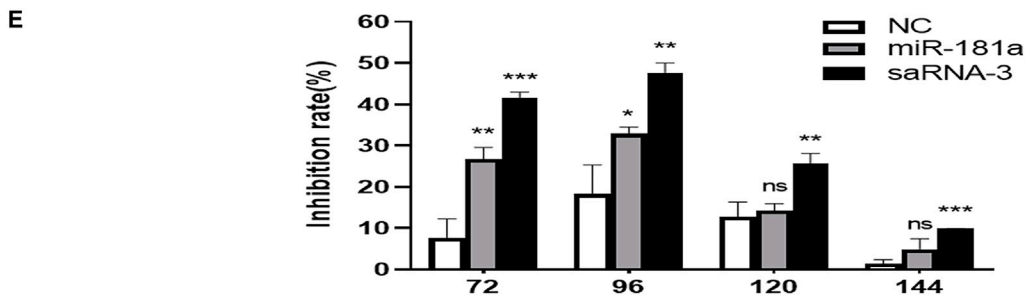
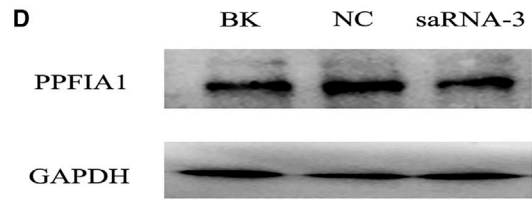
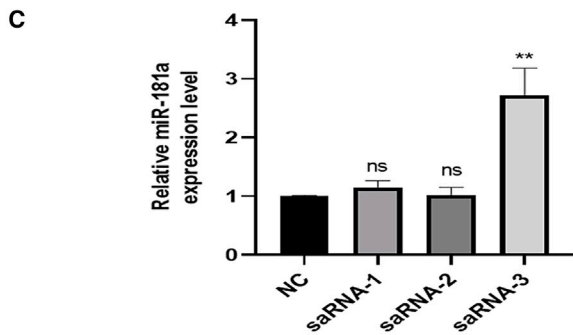
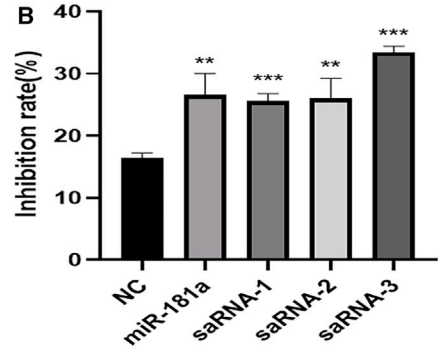
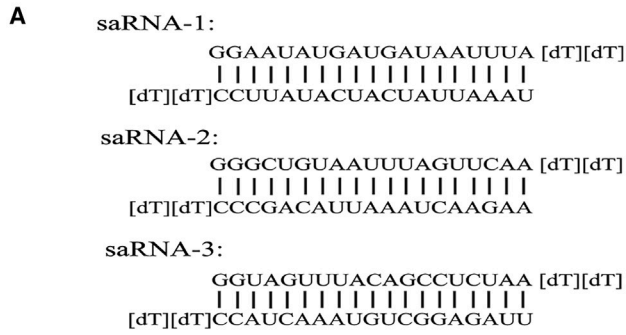
LSCs are a major cause of imatinib resistance and CML recurrence. The ability of LSCs to persist after TKI treatment and form a reservoir contributes to the recurrence and progression of CML, as well as TKI resistance. LSC quantitation at diagnosis and after treatment can predict patients' response to first-line treatment and their prognosis.^{33,34}

c-kit is a receptor tyrosine kinase expressed in different kinds of stem cells (especially in hematopoietic stem cells), which plays an important role in their maintenance and differentiation.^{35,36} Thus, inhibition of c-kit also inhibits the proliferation of CML stem/progenitor cells.³⁷ c-kit is a cell surface receptor on hematopoietic stem cells and a proto-oncogene. After interacting with its ligand, stem cell factor (SCF), c-kit provides important cellular signals for the survival, proliferation, and differentiation of hematopoietic stem cells and hematopoietic progenitor cells. Therefore, c-kit is a feasible therapeutic target in CML.^{38–40} In the present study, we found that the proportion of c-kit-positive cells was higher in the IMR CML cell population than that in the imatinib-sensitive CML cell population. The tissue expression patterns of c-kit in mice and humans are comparable. Therefore, mice may be an effective model to study the on- and off-target toxicities of anti-c-kit directed immunotherapy.^{41,42} We found that treatment with miR-181a mimic or PPFIA1-siRNA reduced the proportion of c-kit-positive CML cells. miR-181a has been previously shown to inhibit the c-kit pathway and prevent the development of CML.⁴³ It is also reported that SCF/c-kit signaling must be inhibited in order for TKIs to induce the apoptosis of CML cells, since SCF can resist the inhibitory effect of TKIs in CML cells.

We showed that the proportion of CD34-positive cells within the IMR CML cell population was higher than that in the imatinib-sensitive CML cell population. Thus, imatinib resistance may be related to

Figure 3. miR-181a and PPFIA1-siRNA decreased c-kit and CD34 expression on imatinib-resistant chronic myeloid leukemia cells

(A) Phosphorylation of signaling proteins was assessed in the PPFIA1-siRNA and NC groups, using a phosphoantibody microarray system. The difference in phosphorylation sites between the PPFIA1-siRNA and NC groups was expressed as the Phos ratio. The Phos ratio for the c-kit protein decreased most significantly after PPFIA1-siRNA transfection. (B) Flow cytometry showed that the proportion of c-kit⁺ cells in the imatinib-sensitive K562 and KCL22 cell population was lower than that in the imatinib-resistant K562-IMR and KCL22-IMR cell population. After 48 h of treatment with either the miR-181a mimic or PPFIA1-siRNA, the proportion of c-kit⁺ cells within the K562-IMR. Significance was determined by Student's t test, *p < 0.05, **p < 0.01, ***p < 0.001 (C) and KCL22-IMR (D) cell populations decreased, compared with the NC group. This was also confirmed by western blotting. (E) Flow cytometry showed that the proportion of CD34⁺ cells within the K562-IMR and KCL22-IMR cell populations decreased after treatment with miR-181a mimic and PPFIA1-siRNA for 48 h, compared with the NC. The data are presented as the mean ± SD, obtained from at least three independent experiments. Significance was determined by Student's t test, *p < 0.05, **p < 0.01, ***p < 0.001 versus the NC group.



(legend on next page)

the increase in the number of LSCs. After treatment with miR-181a mimic or *PPF1A1*-siRNA, the proportion of CD34-positive cells decreased. The expression of miR-181a is low in LSCs. Moreover, miR-181a has been shown to inhibit the proliferation of LSCs *in vitro* and the development of leukemia *in vivo* by targeting SERPINE1. Therefore, miR-181a is a potential therapeutic agent for targeting LSCs. A study showed that after 12 months of treatment with imatinib, the percentage of CD34⁺c-kit⁺ cells in CML patients with a complete cytogenetic response or a major molecular response, which are associated with disease improvement, decreased significantly. Therefore, to obtain the best treatment response in CML patients, it is necessary to eliminate CD34⁺ and c-kit⁺ cells by inducing their apoptosis. These results show that the success of treatment in CML is affected by the frequencies of CD34⁺ and c-kit⁺ CML cells.⁴⁴

Apoptosis is catalyzed by thousands of proteins and requires the enzymatic activity of effector caspases.⁴⁵ Inducing apoptosis by stimulating exogenous signaling pathways can overcome resistance to therapeutic drugs.^{46,47} A better understanding of drug-resistant molecules (and the underlying mechanisms) will help to design clinically successful cancer treatment strategies, especially in patients with disease recurrence. For example, the continuous activation of the MEK signaling cascade emphasizes the importance of auxiliary pathways, independent of the BCR-ABL1 fusion protein activation, in the development of future therapies targeting residual LSCs and drug-resistant patients lacking the BCR-ABL1 mutation.⁴⁸

Gene activation by saRNAs involves the targeted recruitment of the Argonaute protein to specific promoter sequences, which then induces stable epigenetic changes to promote transcription. Meanwhile, RNAi involves the RNA-induced silencing complex, which inhibits gene expression by catalyzing the degradation of complementary mRNA. saRNA is also an Ago-dependent process (involving mainly Ago2 and Ago1), which involves the delayed initiation and sustained activity across multiple cell divisions. These characteristics are in sharp contrast to those of RNAi, indicating that epigenetic mechanisms are involved.¹⁸ To find saRNAs targeting *PPF1A1*, we interrogated the promoter region of miR-181a (selected 1,000 bp) using the Ensembl database, and we generated complementary sequences 19 bp in length, with two additional suspended nucleotides ([dT] [dT], required for binding the target sequence). saRNA activation begins

in the same way as RNAi in the cytoplasmic Ago pathway; however, it becomes different from the RNAi process after Ago is programmed by the guiding RNA, which targets a nuclear promoter sequence. Therefore, RNA activation has common characteristics with RNAi, such as Ago dependence, and also has unique characteristics such as delayed dynamics and longer persistence.⁴⁹

RNA activation is a nuclear process. Thus, a higher concentration of saRNA is required to achieve the same effects in cultured cells as that of siRNA to induce cytoplasmic RNAi. Higher concentrations of nuclear RNA activation and RNAi are necessary to compensate for the inherent nuclear rejection characteristics of double-stranded RNA.⁵⁰ When the saRNA targeting the miR-181a promoter acts on CML cells, under the condition of increasing the same concentration, the cell viability is detected within 72–144 h. We observed that the inhibition of CML cell proliferation by saRNA was more potent and lasted longer than that of miR-181a. This delayed kinetics may obtain its nuclear target through saRNA, and the subsequent gene induction involving histone modification represents a rate limiting step. Another feature of RNA activation is that the effect is prolonged after a single transfection of saRNA, which may last for over 10 days.⁵¹ saRNA has important applications in the fields of gene reprogramming and gene therapy, and it can also be used for cell-based brain repair and the treatment of gene expression defects in neurological diseases. Thus, there is potential to use saRNA as a scalable tool for the treatment of haploid deficiency in neuropathogenesis.

In conclusion, we identified an saRNA (saRNA-3), which promoted the production of endogenous pri-miR-181a. The resulting increase in endogenous miR-181a levels overcame BCR-ABL-independent imatinib resistance better than the exogenous miR-181a mimic by inhibiting LSC self-renewal and promoting their apoptosis by targeting *PPF1A1*.

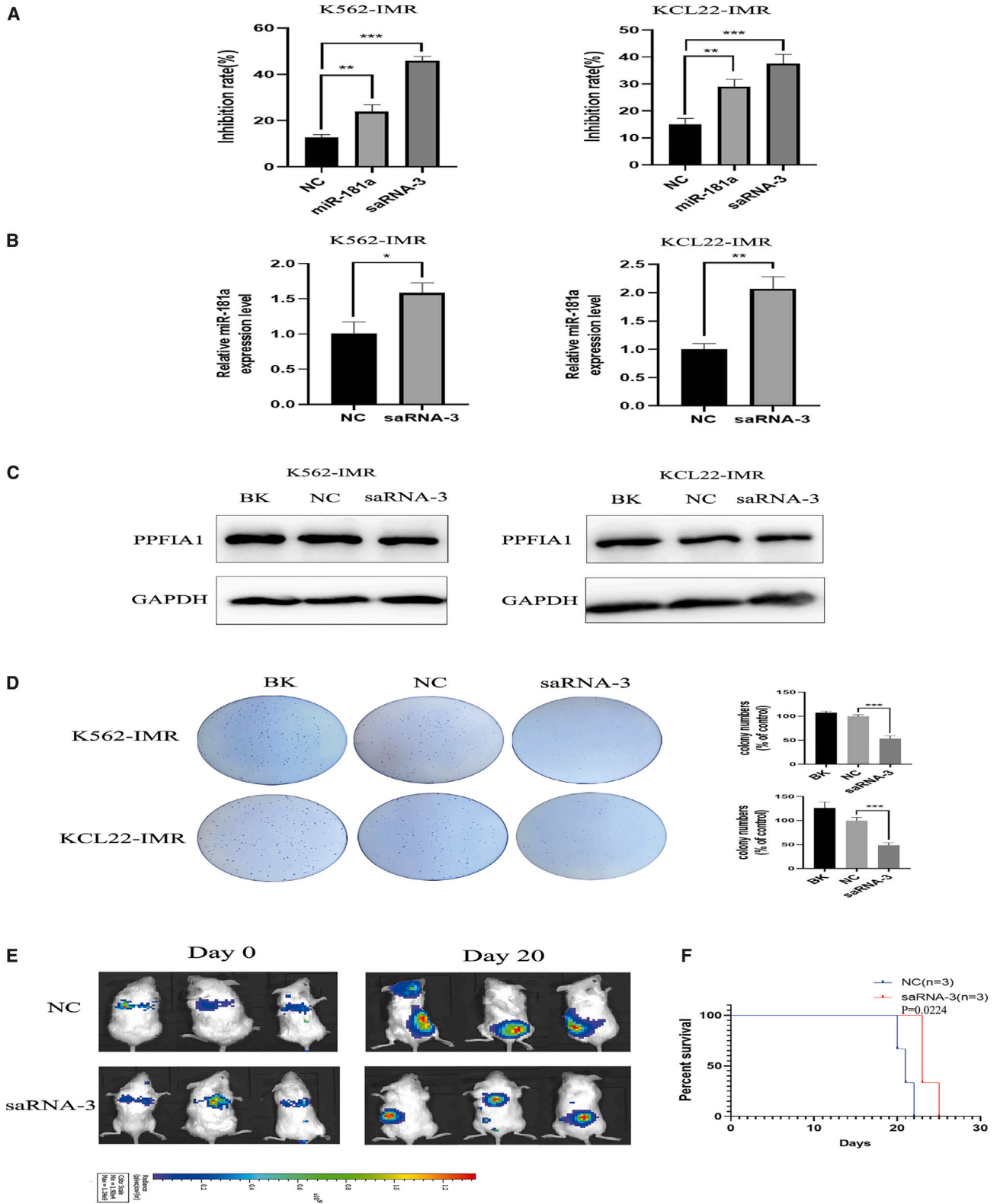
MATERIALS AND METHODS

saRNA and sequences

In humans, miR-181a1 and miR-181a2 are located on chromosome 1 (bp 198,859,04–198,859,153) and chromosome 2 (bp 124,692,442–124,692,551), respectively. saRNAs target the miR-181a promoter, similarly to siRNAs. saRNA is 19 bp in length, with a sequence complementary to the miR-181a promoter, and the suspended two

Figure 4. The newly identified saRNA-3 inhibited chronic myeloid leukemia cell proliferation more strongly than miR-181a

(A) The strategy used to identify the promoter region of the activated target genes and design saRNAs using the Ensembl (<http://www.ensembl.org>) genome browser. The sequences of three saRNAs (named saRNA 1–3) are shown. (B) The inhibitory effect of 200 nM saRNA 1–3 on the proliferation of K562 cells 72 h after transfection was compared with the NC; viability was detected using the CCK-8 assay. All the saRNAs inhibited the proliferation of K562 cells, but only saRNA-3 had a stronger inhibitory effect than the miR-181a mimic. (C) The expression level of miR-181a in K562 cells was detected 72 h after the transfection of RNAs 1–3. Only saRNA-3 could increase the endogenous expression of miR-181a. (D) The effect of transfecting K562 cells saRNA-3 for 72 h on the expression of *PPF1A1* protein was assessed by western blotting. After saRNA-3 transfection, *PPF1A1* protein expression (targeted by miR-181a) decreased, compared with the NC group. (E) After transfection with saRNA-3 at a concentration of 200 nM, the inhibition of cell proliferation was detected using the CCK-8 assay at 72, 96, 120, and 144 h. saRNA-3 had a stronger inhibitory effect on the proliferation of K562 cells than the miR-181a mimic at all the time points. At 120 and 144 h, the effect of the miR-181a mimic was not significantly different from that of the NC. By contrast, saRNA-3 significantly inhibited the proliferation of K562 cells, compared with the NC. (F) Compared with NC group, saRNA-3 also inhibited the colony formation capacity of K562 cells in soft agar; while, no significant difference in colony formation was observed between the BK and NC groups. 5,000 cells per well were plated into 6-well plates. The data are presented as the mean ± SD, obtained from at least three independent experiments. Significance was determined by Student's t test, *p < 0.05, **p < 0.01, ***p < 0.01 versus the NC.



(legend on next page)

nucleotides ([dT][dT]). Negative control, sense: 5'-UUCUCCGAAC GUGUCACGUTT-3' and antisense: 5'-ACGUGACACGUUCGGA GATT-3'. *PPF1A1*-siRNA, sense: 5'-CCACAAAGCUCUGGAUGAA dTdT-3' and antisense: 5'-UUCAUCCAGAGCUUUGUGGdTdT-3'. *PPF1A1* 3' UTR, 5'-UUUUAGUCUUUCAAUUGAAUGUA-3'. *PPF1A1*-mut-3' UTR, 5'-UUUUAGUCUUUCAAUUGAAUGUA-3'. miR-181a mature sequence, 5'-AACAUUCAACGCUGUCGGUGA GU-3' miR181a mimic sense, 5'-AACAUUCAACGCUGUCGGUG AGU-3' and antisense, 5'-UCACCGACAGCGUUGAAUGUUG U-3' saRNA-1, sense: 5'-GGAAUUGAUGAUAUUUAdTdT-3' and antisense: 5'-UAAAUAUCAUCAUUCcDTdT-3'. saRNA-2, sense: 5'-GGCUGUAAUUUAGUUCAdTdT-3' and antisense: 5'-UUGAACUAAAUAACAGCCcDTdT-3'. saRNA-3, sense: 5'-GG UAGUUUACAGCCUCUAAAdTdT-3' and antisense: 5'-UUAGAG GCUGUAAACUACCcDTdT-3'.

Cell culture and transfection

The K562 cell line was purchased from the Shanghai Institute of Cell Biology, China. The KCL22 cell line was kindly provided by Professor Markus Muschen (Children's Hospital Los Angeles, Los Angeles, CA, USA). K562-IMR and KCL22-IMR cells, resistant to 1 μ M imatinib, were constructed in our laboratory by continuous exposure to increasing concentrations of imatinib. K562-IMR/luciferase cells were constructed by stable transfection; efficient and stable firefly luciferase expression was confirmed. Briefly, the cells were diluted with the serum-free and antibiotic-free RPMI-1640 medium. The Lipofectamine 2000 reagent was gently mixed in a 1:1 (v/v) ratio with nucleic acid and incubated for 20 min at room temperature. The Lipofectamine 2000-RNA complex was then slowly added to the cell suspension, followed by gentle plate agitation, until fully mixed. Next, RPMI-1640 medium supplemented with 20% fetal bovine serum (FBS) was added to each well of cells. On culture completion, 20 μ L CCK-8 reagent was added to each well, followed by a 1 h incubation, to determine cell viability. Absorbance was measured at 450 nm, using a multi-functional microplate reader.

Soft agar colony formation assay

After counting, the cells were diluted with serum-free and antibiotic-free RPMI-1640 medium and inoculated into 96-well plates at 5,000 cells in 50 μ L per well. Lipofectamine 2000, diluted in reduced-serum medium Opti-MEM, was mixed with small nucleic acids (also pre-diluted in Opti-MEM) at a ratio of 1:1 (v/v), followed by a 5-min in-

ubation at room temperature. Lipofectamine 2000/nucleic acid mixture was then slowly added to cell suspension, followed by a 20-min incubation at room temperature. The transfection was completed after 6 h at 37°C, 5% CO₂. Next, 1.2% warm soft agarose solution and warm 20% FBS 1640 medium were mixed. 1 mL of the mixture (containing 0.6% soft agarose gel solution and 10% FBS 1640 medium) was then added to each well of a 6-well plate and cooled to solidify the lower gel. Cell suspensions were collected 6 h after small nucleic acid transfection. The cells in each well were mixed with 1 mL of the agarose gel mixture (containing 0.4% soft agarose gel solution and 10% FBS 1640 medium). After cooling and solidification, the 6-well plate contained cells suspended in a gel matrix. The 6-well plate was placed in the incubator for cell culture. When clone formation was observed, the glue plane was cleaned three times with phosphate-buffered saline (PBS). The cells were fixed for 30 min with the addition of 500 μ L 4% paraformaldehyde solution to each well, and the glue plane was washed with PBS three times. Clones were stained with the addition of 1 mL 0.005% crystal violet dye to each well. The dye was washed away with PBS, and the number of clones in each experimental group was assessed.

RNA immunoprecipitation assay

miR-181a and NC miRNA were transfected individually into K562-IMR cells. After transfection, the cells were collected and washed with PBS. Cells were lysed in RIPA lysis buffer and quantified. An anti-Ago2 antibody was added to the miR-181a mimic and NC-transfected cells (at a lysate to antibody ratio of 1:100) and incubated on a rotator at 4°C overnight. The same volume of protein A/G beads was then added to each of the test groups and incubated on a rotator at 4°C for 4 h. The protein A/G beads were then collected and incubated with PBS (containing protease K) at 55°C for 30 min. RNA was extracted from the two groups, and *PPF1A1* mRNA was detected by qPCR.

Real-time quantitative PCR

Total RNA was extracted from cells with TRIzol reagent and transformed into cDNA after reverse transcription. The cDNA template was then combined with primers, the SYBR Green Mix, and RNase-free water. After about 40 cycles of the real-time qPCR reaction, cycle threshold (Ct) values were recorded on the Bio-Rad CFX96 real-time PCR detection system. The RNA expression levels were normalized to those of the internal reference, and the fold-changes in RNA expression levels were calculated using the $2^{-\Delta\Delta Ct}$ method.

Figure 5. saRNA increased miR-181a expression to overcome the imatinib resistance of chronic myeloid leukemia cells *in vitro* and *in vivo*

(A) The inhibitory effect of saRNA-3 on cell proliferation was also validated in K562-IMR, using the CCK-8 assay. 72 h after transfection, 200 nM saRNA-3 repressed the proliferation of K562-IMR cells more strongly than the miR-181a mimic. (B) Quantitative real-time PCR was used to show that the expression of miR-181a was increased in K562-IMR and KCL22-IMR cells 72 h after transfection with 200 nM saRNA-3, compared with the NC. (C) After 72 h of saRNA-3 transfection, a decrease in the expression level of *PPF1A1* (compared with the NC), a target of miR-181a, was detected by western blotting in K562-IMR and KCL22-IMR cells. (D) saRNA-3 inhibited the colony formation capacity of K562-IMR and KCL22-IMR cells, compared with the NC; there was no significant difference between the colony formation results of the BK and NC groups. (E) B-NDG mice received K562-IMR/luciferase cells via infection of the tail vein. These mice were then treated with equal volumes of 10 nmol NC or 10 nmol saRNA-3 every other day for 10 days. The diffusion of K562-IMR/luciferase cells in the B-NDG mice after treatment was then observed in each group (n = 3 per group). (F) saRNA-3 prolonged the survival time of B-NDG mice, compared with the NC. The data are presented as the mean \pm SD, obtained from at least three independent experiments. Significance was determined by Student's t test, *p < 0.05, **p < 0.01, ***p < 0.001 versus the NC group.

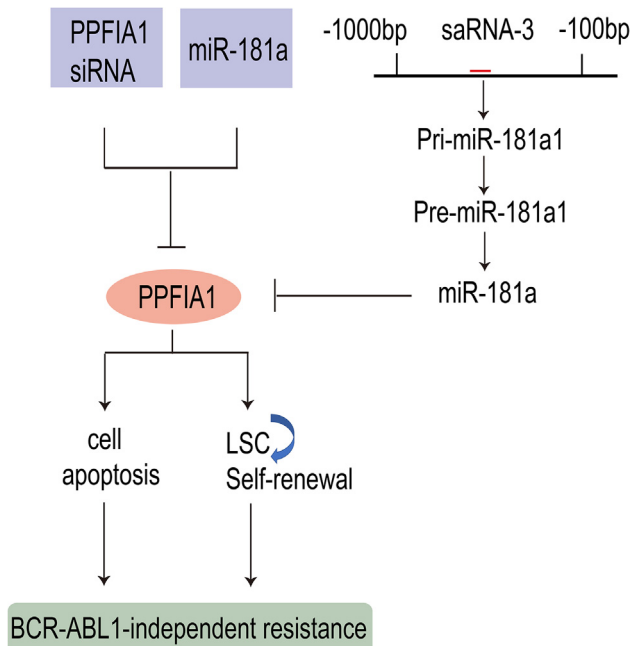


Figure 6. A schematic diagram outlining the role of saRNA in BCR-ABL1-independent imatinib-resistant chronic myeloid leukemia

Targeting *PPFIA1* expression with *PPFIA1*-siRNA or miR-181a can overcome BCR-ABL1-independent imatinib resistance by inhibiting leukemic stem cell proliferation and promoting their apoptosis. saRNA-3 overcomes imatinib resistance in chronic myeloid leukemia by activating the production of endogenous miR-181a.

Western blotting

Firstly, total protein was extracted from each group of cells with RIPA lysis buffer and quantified using a BCA kit. Protein samples were mixed with 5× protein loading buffer and denatured to 100°C for 10 min. Equal amounts of protein were separated on a 10% SDS-PAGE resolving gel (with a 5% stacking gel) by electrophoresis at 120 V (80 V for the stacking gel). A polyvinylidene fluoride (PVDF) membrane was prepared by soaking in methanol and then blotting in blotting buffer. The proteins were transferred from the gel to the PVDF membrane. The PVDF membrane was blocked with 5% skim milk for 1–2 h at room temperature on a decolorizing shaker. After a washing step, the PVDF membrane was treated with a primary antibody against the target protein and an isotype control and incubated overnight at 4°C on a shaker. The PVDF membrane was then washed and treated and incubated with secondary antibodies at room temperature for 1–2 h on a decolorizing shaker. The Immobilon Western HRP luminescent solution was prepared and added to the PVDF membrane. Finally, the PVDF membrane was imaged on a gel imaging system.

Phosphate-specific protein microarray

After transfection of *PPFIA1*-siRNA, the cells were collected and washed with PBS and pelleted by centrifugation. Total protein was then extracted from the cell pellets. Proteins of the same quality were labeled with biotin and then hybridized with the pre-phosphorylation array using an antibody array kit (Full Moon BioSystems,

USA). This is used to detect the phosphorylated antibody spectrum of site-specific cancer signals. The fluorescence intensity of the proteins was then measured. The ratio of phosphorylated to unphosphorylated (Phos ratio) was calculated as follows: amount of phosphorylated protein/amount of unphosphorylated protein.

Comparison of CD34⁺/c-kit⁺ ratios by flow cytometry

Equal numbers of cells were placed in flow cytometry tubes and washed with PBS by centrifugation at 800 rpm for 3 min. Flow cytometry antibodies (anti-human CD34-APC and anti-human c-kit-FITC [both from Biotend]) were then added to each cell pellet (at an antibody to staining buffer ratio of 1:100), and the cells were incubated for 30–45 min on ice in the dark. Next, the cells were washed twice with 1 mL PBS by centrifugation at 800 rpm for 3 min. The cells were resuspended in 200 μL PBS, and we transferred the cell suspension to a 96-well plate for acquisition on a BD FACSVerser flow cytometer (BD Biosciences).

Human K562-IMR/luciferase transplanted animal model

4-week-old B-NDG (NOD.CB17-Prkdcscid IL2rgtm1/Bcgen) mice were acquired from the Beijing Biocytogen Company and raised by The Animal Experiment Management Center of Jinan University. All animal experiments were approved by and conformed to the relevant regulatory standards of the Institutional Animal Care and Use Committee at the Institute of Laboratory Animal Science, Jinan University (Guangzhou, China). 2 weeks after isolation, 1×10^6 K562-IMR/luciferase cells were injected into the tail vein of each B-NDG mouse. On day 0, *in vivo* imaging was performed on each B-NDG mouse. On day 10, B-NDG mice in each group were treated after onset. 40 mice were randomly divided into two large groups (K562 group and K562-IMR group). A large group was divided into four groups of three. The B-NDG mice were treated with imatinib and then injected with 10 nmol NC solution, 10 nmol *PPFIA1*-siRNA solution, or 10 nmol miR-181a mimic solution. The other large group of mice was divided into two groups of three; one group was injected with 10 nmol NC solution, and the other group was injected with 10 nmol saRNA-3 solution. The B-NDG mice were given imatinib every other day after developing CML. At the end of the treatment period, proliferation and metastasis of K562-IMR/luciferase cells in mice were evaluated by *in vivo* imaging. The survival times and body weights of the B-NDG mice were recorded, and survival curves were generated for mice in different experimental groups.

Statistical analysis

All statistical analyses were performed using GraphPad Prism 8.0.1 software. The results were expressed as the mean ± standard deviation (SD). Significant differences between groups were determined using one-way analysis of variance with the post-hoc Bonferroni test. Paired analyses were performed using the Student's *t* test. *p* values <0.05 were considered as a measure of statistical significance.

DATA AVAILABILITY

All data associated with this study are presented in the paper or the [supplemental information](#). Materials that support the findings of this study are available from the corresponding author upon request.

SUPPLEMENTAL INFORMATION

Supplemental information can be found online at <https://doi.org/10.1016/j.omtn.2023.04.026>.

ACKNOWLEDGMENTS

The authors offer many thanks to Wayen Biotechnology (Shanghai, China) for phospho-array detection. This work was supported by grants from The State Key Laboratory of Natural and Biomimetic Drugs (grant number K202113), Science and Technology Program of Guangdong Province (grant number 2017B 030303001), and Science and Technology Program of Guangzhou City (grant number 202206010063).

AUTHOR CONTRIBUTIONS

J.F. conceived the study and designed the experiments. C.L., Z.L., Z.W., and R.S. performed the experiments. X.W., Y.L., Z.Y., J.Y., and R.S. analyzed the data. Z.Y. and G.H. provided reagents, materials, and analytical tools. J.F., K.Z., H.H., and H.N. wrote the manuscript.

DECLARATION OF INTERESTS

All authors declare that they have no competing financial interests or personal relationships that could have appeared to influence the work reported in this paper.

REFERENCES

- Minciacchi, V.R., Kumar, R., and Krause, D.S. (2021). Chronic myeloid leukemia: a model disease of the past, present and future. *Cells* 10.
- Ozkan, T., Hekmatshoar, Y., Karabay, A.Z., Koc, A., Altinok Gunes, B., Karadag Gurel, A., and Sunguroglu, A. (2021). Assessment of azithromycin as an anticancer agent for treatment of imatinib sensitive and resistant CML cells. *Leuk. Res.* 102, 106523.
- Alves, R., Gonçalves, A.C., Rutella, S., Almeida, A.M., De Las Rivas, J., Trougakos, I.P., and Sarmiento Ribeiro, A.B. (2021). Resistance to tyrosine kinase inhibitors in chronic myeloid leukemia—from molecular mechanisms to clinical relevance. *Cancers* 13, 4820.
- Cogle, C.R. (2013). Overcoming chronic myeloid leukemia stem cell resistance to imatinib by also targeting JAK2. *J. Natl. Cancer Inst.* 105, 378–379.
- Lu, T.X., and Rothenberg, M.E. (2018). MicroRNA. *J. Allergy Clin. Immunol.* 141, 1202–1207.
- Lee, Y.S., and Dutta, A. (2009). MicroRNAs in cancer. *Annu. Rev. Pathol.* 4, 199–227.
- Choi, E.J., Yun, J.A., Jabeen, S., Jeon, E.K., Won, H.S., Ko, Y.H., and Kim, S.Y. (2014). Prognostic significance of TMEM16A, PPF1A1, and FADD expression in invasive ductal carcinoma of the breast. *World J. Surg. Oncol.* 12, 137.
- Lin, S., Pan, L., Guo, S., Wu, J., Jin, L., Wang, J.C., and Wang, S. (2013). Prognostic role of microRNA-181a/b in hematological malignancies: a meta-analysis. *PLoS One* 8, e59532.
- Zhou, H., Cao, T., Li, W.P., and Wu, G. (2019). Combined expression and prognostic significance of PPF1A1 and ALG3 in head and neck squamous cell carcinoma. *Mol. Biol. Rep.* 46, 2693–2701.
- Astro, V., Chiaretti, S., Magistrati, E., Fivaz, M., and de Curtis, I. (2014). Liprin- α 1, ERC1 and LL5 define polarized and dynamic structures that are implicated in cell migration. *J. Cell Sci.* 127, 3862–3876.
- Che, H., Ding, H., and Jia, X. (2020). circ_0080145 Enhances Imatinib Resistance of Chronic Myeloid Leukemia by Regulating miR-326/PPF1A1 Axis (Cancer Biother Radiopharm).
- Zhou, H., and Xu, R. (2015). Leukemia stem cells: the root of chronic myeloid leukemia. *Protein Cell* 6, 403–412.
- Nicholson, E., and Holyoake, T. (2009). The chronic myeloid leukemia stem cell. *Clin. Lymphoma Myeloma* 9 (Suppl 4), S376–S381.
- Jin, B., Wang, C., Li, J., Du, X., Ding, K., and Pan, J. (2017). Anthelmintic Niclosamide disrupts the interplay of p65 and FOXM1/ β -catenin and eradicates leukemia stem cells in chronic myelogenous leukemia. *Clin. Cancer Res.* 23, 789–803.
- Valent, P. (2008). Emerging stem cell concepts for imatinib-resistant chronic myeloid leukaemia: implications for the biology, management, and therapy of the disease. *Br. J. Haematol.* 142, 361–378.
- Shah, M., and Bhatia, R. (2018). Preservation of quiescent chronic myelogenous leukemia stem cells by the bone marrow microenvironment. *Adv. Exp. Med. Biol.* 1100, 97–110.
- Rice, K.N., and Jamieson, C.H.M. (2010). Molecular pathways to CML stem cells. *Int. J. Hematol.* 91, 748–752.
- Guo, D., Barry, L., Lin, S.S.H., Huang, V., and Li, L.-C. (2014). RNAa in action: from the exception to the norm. *RNA Biol.* 11, 1221–1225.
- Setten, R.L., Lightfoot, H.L., Habib, N.A., and Rossi, J.J. (2018). Development of MTL-CEBPA: small activating RNA drug for hepatocellular carcinoma. *Curr. Pharmaceut. Biotechnol.* 19, 611–621.
- Pushparaj, P.N., Aarthi, J.J., Kumar, S.D., and Manikandan, J. (2008). RNAi and RNAa—the yin and yang of RNAome. *Bioinformation* 2, 235–237.
- Portnoy, V., Huang, V., Place, R.F., and Li, L.C. (2011). Small RNA and transcriptional upregulation. *Wiley Interdiscip. Rev. RNA* 2, 748–760.
- Kwok, A., Raulf, N., and Habib, N. (2019). Developing small activating RNA as a therapeutic: current challenges and promises. *Ther. Deliv.* 10, 151–164.
- Li, C., Jiang, W., Hu, Q., Li, L.C., Dong, L., Chen, R., Zhang, Y., Tang, Y., Thrasher, J.B., Liu, C.B., and Li, B. (2016). Enhancing DPYSL3 gene expression via a promoter-targeted small activating RNA approach suppresses cancer cell motility and metastasis. *Oncotarget* 7, 22893–22910.
- Huan, H., Wen, X., Chen, X., Wu, L., Liu, W., Habib, N.A., Bie, P., and Xia, F. (2016). C/EBP α short-activating RNA suppresses metastasis of hepatocellular carcinoma through inhibiting EGFR/ β -Catenin signaling mediated EMT. *PLoS One* 11, e0153117.
- Zhou, L.Y., He, Z.Y., Xu, T., and Wei, Y.Q. (2018). Current advances in small activating RNAs for gene therapy: principles, applications and challenges. *Curr. Gene Ther.* 18, 134–142.
- Zheng, B., Mai, Q., Jiang, J., and Zhou, Q. (2019). The therapeutic potential of small activating RNAs for colorectal carcinoma. *Curr. Gene Ther.* 19, 140–146.
- Guo, S., Li, K., Hu, B., Li, C., Zhang, M., Hussain, A., Wang, X., Cheng, Q., Yang, F., Ge, K., et al. (2021). Membrane-destabilizing ionizable lipid empowered imaging-guided siRNA delivery and cancer treatment. *Explorations* 1, 35–49.
- Hu, B., Li, B., Li, K., Liu, Y., Li, C., Zheng, L., Zhang, M., Yang, T., Guo, S., Dong, X., et al. (2022). Thermostable ionizable lipid-like nanoparticle (iLAND) for RNAi treatment of hyperlipidemia. *Sci. Adv.* 8, eabm1418.
- Xiong, Y., Ke, R., Zhang, Q., Lan, W., Yuan, W., Chan, K.N.I., Roussel, T., Jiang, Y., Wu, J., Liu, S., et al. (2022). Small activating RNA modulation of the G protein-coupled receptor for cancer treatment. *Adv. Sci.* 9, e2200562.
- Liu, R., Luo, C., Pang, Z., Zhang, J., Ruan, S., Wu, M., Wang, L., Sun, T., Li, N., Han, L., et al. (2023). Advances of nanoparticles as drug delivery systems for disease diagnosis and treatment. *Chin. Chem. Lett.* 34, 107518.
- Singh, P., Kumar, V., Gupta, S.K., Kumari, G., and Verma, M. (2021). Combating TKI resistance in CML by inhibiting the PI3K/Akt/mTOR pathway in combination with TKIs: a review. *Med. Oncol.* 38, 10.
- Wang, G., Zhao, R., Zhao, X., Chen, X.I., Wang, D., Jin, Y., Liu, X.I., Zhao, C.I., Zhu, Y., Ren, C., et al. (2015). MicroRNA-181a enhances the chemotherapeutic sensitivity of chronic myeloid leukemia to imatinib. *Oncol. Lett.* 10, 2835–2841.
- Fathy El-Metwaly, N., Aref, S., Ayed, M., Abdel Hamid, M., and El-Sokkary, A.M.A. (2021). CD34+/CD38- stem cell burden could predict chronic myeloid leukemia patients' outcome. *Asian Pac. J. Cancer Prev. APJCP* 22, 3237–3243.

34. Ma, W., Liu, J., Xie, J., Zhang, X., Zhou, H., Yao, H., Zhang, W., Guo, D., Zhu, L., Xiao, L., et al. (2015). Modulating the growth and imatinib sensitivity of chronic myeloid leukemia stem/progenitor cells with pullulan/MicroRNA nanoparticles in vitro. *J. Biomed. Nanotechnol.* *11*, 1961–1974.
35. Wang, W.L., Conley, A., Reynoso, D., Nolden, L., Lazar, A.J., George, S., and Trent, J.C. (2011). Mechanisms of resistance to imatinib and sunitinib in gastrointestinal stromal tumor. *Cancer Chemother. Pharmacol.* *67* (Suppl 1), S15–S24.
36. Abbaspour Babaei, M., Kamalidehghan, B., Saleem, M., Huri, H.Z., and Ahmadipour, F. (2016). Receptor tyrosine kinase (c-Kit) inhibitors: a potential therapeutic target in cancer cells. *Drug Des. Dev. Ther.* *10*, 2443–2459.
37. Corbin, A.S., O'Hare, T., Gu, Z., Kraft, I.L., Eiring, A.M., Khorashad, J.S., Pomicter, A.D., Zhang, T.Y., Eide, C.A., Manley, P.W., et al. (2013). KIT signaling governs differential sensitivity of mature and primitive CML progenitors to tyrosine kinase inhibitors. *Cancer Res.* *73*, 5775–5786.
38. Pang, W.W., Czechowicz, A., Logan, A.C., Bhardwaj, R., Poyser, J., Park, C.Y., Weissman, I.L., and Shizuru, J.A. (2019). Anti-CD117 antibody depletes normal and myelodysplastic syndrome human hematopoietic stem cells in xenografted mice. *Blood* *133*, 2069–2078.
39. Moore, S., Haylock, D.N., Lévesque, J.P., McDiarmid, L.A., Samels, L.M., To, L.B., Simmons, P.J., and Hughes, T.P. (1998). Stem cell factor as a single agent induces selective proliferation of the Philadelphia chromosome positive fraction of chronic myeloid leukemia CD34(+) cells. *Blood* *92*, 2461–2470.
40. Yasuda, A., Sawai, H., Takahashi, H., Ochi, N., Matsuo, Y., Funahashi, H., Sato, M., Okada, Y., Takeyama, H., and Manabe, T. (2006). The stem cell factor/c-kit receptor pathway enhances proliferation and invasion of pancreatic cancer cells. *Mol. Cancer* *5*, 46.
41. Guo, C., Ran, Q., Sun, C., Zhou, T., Yang, X., Zhang, J., Pang, S., and Xiao, Y. (2020). Loss of FGFR3 delays acute myeloid leukemogenesis by programming weakly pathogenic cd117-positive leukemia stem-like cells. *Front. Pharmacol.* *11*, 632809.
42. Russkamp, N.F., Myburgh, R., Kiefer, J.D., Neri, D., and Manz, M.G. (2021). Anti-CD117 immunotherapy to eliminate hematopoietic and leukemia stem cells. *Exp. Hematol.* *95*, 31–45.
43. Gu, C., Liu, Y., Yin, Z., Yang, J., Huang, G., Zhu, X., Li, Y., and Fei, J. (2019). Discovery of the oncogenic Parp1, a target of bcr-abl and a potential therapeutic, in mir-181a/PPF1A1 signaling pathway. *Mol. Ther. Nucleic Acids* *16*, 1–14.
44. Dybko, J., Haus, O., Jazwiec, B., Urbaniak, J., Wozniak, M., Kaczmar-Dybko, A., Urbaniak-Kujda, D., Kapelko-Slowik, K., and Kuliczowski, K. (2014). CD117 (c-kit) expression on CD34+ cells participates in the cytogenetic response to imatinib in patients with chronic myeloid leukemia in the first chronic phase. *Acta Haematol.* *132*, 166–171.
45. Carneiro, B.A., and El-Deiry, W.S. (2020). Targeting apoptosis in cancer therapy. *Nat. Rev. Clin. Oncol.* *17*, 395–417.
46. Mohammad, R.M., Muqbil, I., Lowe, L., Yedjou, C., Hsu, H.Y., Lin, L.T., Siegelin, M.D., Fimognari, C., Kumar, N.B., Dou, Q.P., et al. (2015). Broad targeting of resistance to apoptosis in cancer. *Semin. Cancer Biol.* *35* (Suppl (Suppl)), S78–s103.
47. Pistrutto, G., Triscuoglio, D., Ceci, C., Garufi, A., and D'Orazi, G. (2016). Apoptosis as anticancer mechanism: function and dysfunction of its modulators and targeted therapeutic strategies. *Aging (Albany NY)* *8*, 603–619.
48. Burslem, G.M., Schultz, A.R., Bondeson, D.P., Eide, C.A., Savage Stevens, S.L., Druker, B.J., and Crews, C.M. (2019). Targeting BCR-ABL1 in chronic myeloid leukemia by PROTAC-mediated targeted protein degradation. *Cancer Res.* *79*, 4744–4753.
49. Li, L.C. (2017). Small RNA-guided transcriptional gene activation (RNAa) in mammalian cells. *Adv. Exp. Med. Biol.* *983*, 1–20.
50. Yi, R., Qin, Y., Macara, I.G., and Cullen, B.R. (2003). Exportin-5 mediates the nuclear export of pre-microRNAs and short hairpin RNAs. *Genes Dev.* *17*, 3011–3016.
51. Place, R.F., Noonan, E.J., Földes-Papp, Z., and Li, L.C. (2010). Defining features and exploring chemical modifications to manipulate RNAa activity. *Curr. Pharmaceut. Biotechnol.* *11*, 518–526.